

EFFECTS OF Nd₂O₃ ON THE CRYSTALLIZATION AND PROPERTIES OF GLASS CERAMIC IN Li₂O–K₂O–Al₂O₃–SiO₂–P₂O₅ SYSTEM

Minh N. H. ^{*}, Hung H. T. D., Khoi T. N., Minh Q. D.

*Faculty of Materials Technology, HCMUT–VNUHCM
268 Ly Thuong Kiet Street, Ward 14, District 10, Ho Chi Minh City, Vietnam*

^{*}Email: *hnminh@hcmut.edu.vn*

Received: 30 December 2016; Accepted for publication: 9 March 2017

ABSTRACT

Glass ceramics (GCs), which often contain a small amount of rare earth oxides to improve their performance, are ideal for dental restorative applications. The aim of this study was to investigate the various effects of Nd₂O₃ content (0–1 wt%) on crystallization and properties of GC derived from Li₂O–K₂O–Al₂O₃–SiO₂–P₂O₅ system. The glass blocks were formed from the molten at 1450 °C. Based on the DTA results, the glass samples were experienced by two–stage heat–treatment (600 °C/ 90 min + 720 °C/ 30 min) to change to ingots. After that, the ingot samples were fired in a hot pressing furnace EP3000 at 930 °C for 30 min. The results of powder X–ray diffraction (XRD) indicated that the final GCs contained crystals such as lithium disilicate (Li₂Si₂O₅ or LS₂), lithium metasilicate (Li₂SiO₃ or LS) and the traces of lithium phosphate (Li₃PO₄). With increasing Nd₂O₃ content, the relative amount of LS phase increased slightly while LS₂ phase decreased. However, the final GC containing 0.75 wt% Nd₂O₃ had the highest bending strength at 293 MPa, the lowest chemical solubility and relative high Vicker hardness. These samples had a high degree of crystallization and the highest relative content of desired LS₂ phase.

Keywords: glass ceramic, dental ceramic, lithium disilicate, rare earth oxide, neodymium oxide Nd₂O₃.

1. INTRODUCTION

Glass ceramics (GCs) containing lithium disilicate (Li₂Si₂O₅ or LS₂) as main crystal phase are ideally suitable for multi options of dental restorative applications: esthetic, layer technique, hot pressing or CAD/CAM all–ceramic restoration. Besides Li₂O, SiO₂, these materials also contain Al₂O₃ and K₂O to enhance the chemical durability [1, 2], P₂O₅ as a heterogeneous nucleating agent that promotes volume nucleation of the LS₂ phases [3–6] ... and small amounts of rare earth oxides playing a role as colorants and fluorescent agents [7].

The rare earth elements (La, Ce, Pr, Nd...) now are widely used in GCs because there are a large number of fluorescing states and wavelengths to choose among the 4f electron

configurations. The changes in density, molar volume, hardness, thermal expansion (CTE) and glass transition temperature (T_g) of the glass system L_n -Si-Al-O-N ($L_n = \text{Ce, Nd, Sm, Eu, Dy, Ho and Er}$) were presented by Ramesh et al. [8], the changes of these properties were found to vary linearly with the cationic fields strength or ionic radius of the rare earth modifier. Wang et al. [9] studied the effects of ZrO_2 , La_2O_3 , CeO_2 , Yb_2O_3 and V_2O_5 on the crystallization kinetics, microstructure and mechanical properties of mica GC. The arrangement in order of subsequence of improving crystallization was $\text{ZrO}_2 > \text{V}_2\text{O}_5 > \text{Yb}_2\text{O}_3 > \text{CeO}_2 > \text{La}_2\text{O}_3$. Bighetti et al. [10] investigated the viability of a silica glass containing rare earth oxides as La_2O_3 , Y_2O_3 , CeO_2 (total was 42 wt%), these oxides were used as infiltration agents in different ceramic substrates. The results demonstrated that calculated compressive residual stress (based on CTE of the substrate and glass) enhanced toughness of the glass-infiltrated composites and the application of this glass composition was feasible. Holand and Beall [1] commented that the effects of dopant d or f ions on the color of transparent GC depend on the degree of their partitioning into the crystals as opposed to remaining in the residual glassy phase.

In fact, there have been some crystallization studies on LS_2 GC that contain a certain amount of rare earth oxides in the compositions [11–13]. Nevertheless, the influences of those oxides' content were not found in these papers.

In this study, the effects on crystallization and the properties of GC derived from the base glass of $\text{Li}_2\text{O-K}_2\text{O-Al}_2\text{O}_3\text{-SiO}_2\text{-P}_2\text{O}_5$ system with different Nd_2O_3 content (0–1 wt%) were investigated.

2. MATERIALS AND METHODS

2.1. Melting base glass

Glass batches were prepared by mixing powder of SiO_2 (Precipitated Silica, Toxolux-Korea); Li_2CO_3 , Al(OH)_3 , KH_2PO_4 , K_2CO_3 (Guangdong Guanghua Chemical Factory Co., Ltd. - China) and Nd_2O_3 (Institute for Technology of Radioactive and Rare Elements (ITRRE) - Vietnam Atomic Energy Institute (VINATOM)). The chemical composition of the base glass was (wt%): Li_2O 17.04, K_2O 3.12, Al_2O_3 3.41, SiO_2 74.05, P_2O_5 2.39. Nd_2O_3 was added in base glass with the content of 0, 0.25, 0.50, 0.75 and 1.00 wt%, The samples were denoted as N-0, N-0.25, N-0.50, N-0.75 and N-1.00. The glass batches were melted at 1450 °C for 90 minutes in platinum crucibles and casted into preheated stainless steel molds to form transparent glass blocks.

The glass blocks were annealed inside a furnace at 450 °C for an hour, then cooled slowly to room temperature to decrease the internal stress in glass.

2.2. Heat treatment

The base glass blocks were milled and sieved through a mesh 325 (45 μm). The fine glass powders were heated from 30 °C to 1050 °C with a heating rate of 10 °C/min in differential thermal analyzer DTA (Perkin Elmer, DTA7, Massachusetts, USA, at Department of Materials Engineering, Faculty of Engineering, Kasetsart University, Thailand). $\alpha\text{-Al}_2\text{O}_3$ powder was used as the reference material.

From the results of DTA, the two-stage heat treatment process was conducted at 600 °C for 90 minutes and 720 °C for 30 minutes to crystal nucleation and crystal growth of the glass

blocks to form GC ingots. Subsequently, these ingots were sintered at 930 °C or hot pressed at 965 °C using EP3000 pressing furnace to produce final GCs.

2.3. Characterization techniques

The phases of glasses and GCs were characterized by powder X-ray diffraction XRD (Bruker D8-Advance, at Institute of Applied Materials Science – Vietnam Academy of Science and Technology (VAST)) with CuK α radiation and 2 θ scanning from 10° to 70° at step size 0.01°, mean time per step was 16.38 s. The integrated intensity (I) of the diffraction lines from any phase in a mixture is proportional to the mass of phase present in the sample [14]. Therefore, the semi quantitative analysis of crystallinity and the crystalline phases can be calculated and assessed by the number, position and intensity of peaks by using a powdery X-ray diffraction pattern general analysis software X'Pert HighScore Plus. Degree of crystallinity was estimated by the ratio [15]:

$$\% \text{ Crystallinity} = \frac{\text{Sum of net area}}{(\text{Sum of net area})+(\text{Sum of background area})} \times 100\% \quad (1)$$

Crystallite sizes (nm) of LS₂ phase can be calculated via Scherrer's equation, using the maximum peak at hkl [111] (2 θ \approx 24.8°):

$$\text{Crystallite size} = \frac{K\lambda}{(FWHM) \cos \theta} \quad (2)$$

where K is the Scherrer constant and is 0.9 [16]; λ is the X-ray diffraction wavelength and is 0.154 nm; $FWHM$ is the full width at half its maximum intensity (an angular width, in terms of 2 θ); θ is the Bragg angle (in radians).

Each group consisted of ten final GC rods was ground and polished by SiC papers (240, 600, 1200 and 2500–grit) to create smooth and parallel faces, then cleaned in ultra-sonic bath for 5 minutes and dried before properties testing. The dimensions of the bar-shaped samples after polishing were about 40 x 8 x 4 (mm).

Three-point bending strength was tested by Testometric M350–10CT equipment (England) at Faculty of Materials Technology (HCMUT–VNUHCM), referred to the ISO 6872–2008 [17]. Vicker hardness was tested by Highwood–HWMMT–X3 equipment (Japan) at Materials Technology Laboratory (HCMUT–VNUHCM) with the 4 x 8 x 15 (mm) bars, referred to ASTM C1327–99 [18]. The chemical solubility test method was referred to the ISO 6872–2008 (the mass loss in $\mu\text{g}/\text{cm}^2$ after immersed in 4 vol% acetic acid solution at 80 \pm 3 °C for 16 h).

Color measurements were made by CR–300 Chroma Meter (Konica Minolta – Japan) at Faculty of Chemical Engineering (HCMUT–VNUHCM). The colorimetric effects of Nd₂O₃ additions in the range used on the CIE L*a*b* color parameters of GC. The CIE L*a*b* color difference, ΔE^* , was calculated [19] between the blank sample N–0 and the Nd₂O₃–containing samples.

$$\Delta E^* = [(\Delta L^*)^2 + (\Delta a^*)^2 + (\Delta b^*)^2]^{1/2} \quad (3)$$

where:

ΔE^* : the CIE unit of color difference,

L_c^*, a_c^*, b_c^* : the CIE color parameters of the Nd₂O₃-containing specimens.

$$\Delta L^* = L_c^* - L_n^* \quad (4)$$

$$\Delta a^* = a_c^* - a_n^* \quad (5)$$

$$\Delta b^* = b_c^* - b_n^* \quad (6)$$

L_n^*, a_n^*, b_n^* : the CIE color parameters of the samples without Nd_2O_3 (N=0).

The microstructure of GCs was analyzed by scanning electron microscope (SEM– Philips XL30, at Department of Materials Engineering, Faculty of Engineering, Kasetsart University, Thailand). Fracture surfaces of samples were not etched, polished surfaces were etched in 10 vol% HF solution for 10 seconds and then Au sputtered.

3. RESULTS AND DISCUSSION

3.1. The results of DTA

The DTA curves of the glasses are demonstrated in Figure 1. The glass transition temperature is denoted by T_g , at which the sample changes from solid to liquid behaviour. The clear exothermic peak T_c is determined for crystallization and the endothermic peak T_m showed the melting point. Regarding to the use of Nd_2O_3 in raw mixture, they show small variation of characteristic temperatures of glass powders N=0, N=0.25, N=0.50, N=0.75, N=1.00 (Table 1).

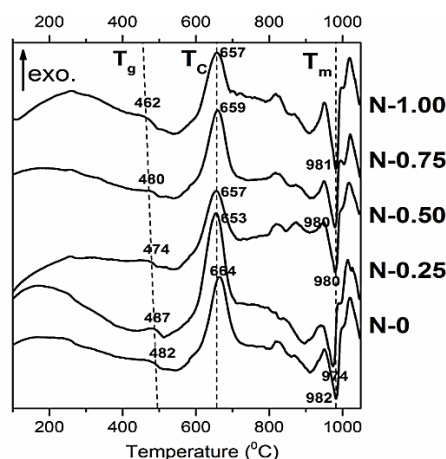


Figure 1. DTA analysis of basic glasses.

Table 1. Characteristic temperature of glass powders N=0, N=0.25, N=0.50, N=0.75, N=1.00 analyzed by DTA.

Sample	T_g (°C)	T_c (°C)	T_m (°C)
N=0	482	664	982
N=0.25	487	653	974
N=0.50	474	657	980
N=0.75	480	659	980
N=1.00	462	657	981

3.2. The results of XRD analysis

The XRD patterns of glass group N=0 are represented in Figure 2. The degree of crystallinity, calculated by equation (1), and characteristic peaks of N=0 in different states are shown in Table 2. It is indicated that, the LS and LS_2 crystals were crystallized from the samples

undergoing the first preheat treatment at 600 °C. After the second stage and sintering step, there had been the rise in the intensity of LS_2 peaks as opposed to the decline of LS peaks, this demonstrates that the LS crystals continuously react with silica through a solid-state reaction to form LS_2 crystals. Li_3PO_4 crystals can be detected after being fired in hot pressing furnace at 930 °C.

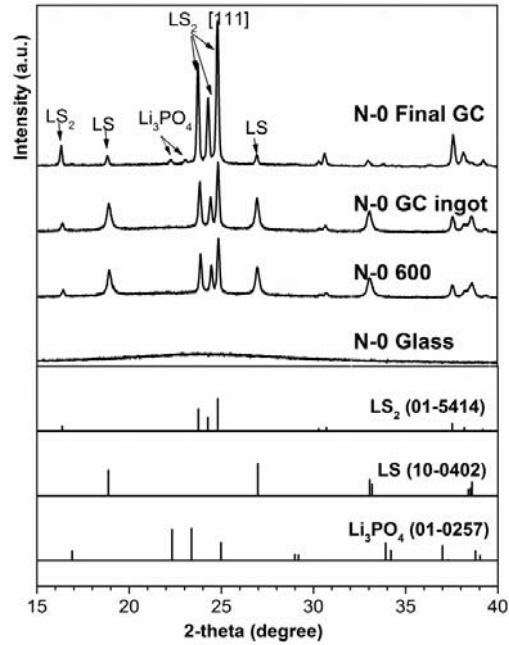


Figure 2. XRD patterns of N-0 in different states.

Table 2. Degree of crystallinity and characteristic peaks of N-0 in different states.

State of N-0	Degree of crystallinity (%)	Intensities of main XRD peaks (cts)		
		LS_2	LS	Li_3PO_4
Glass	–			–
600	24	1670	820	–
GC ingot	28	1963	902	144
Final GC	37	4351	333	137

Consequently, the crystallization process of this GC system can be inferred, as follow:

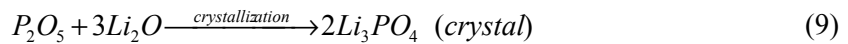
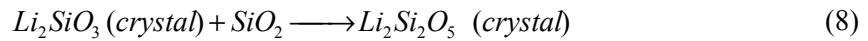
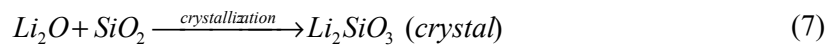


Figure 3 is the results of a semi-quantitative analysis by the intensity values of main peaks of XRD of the LS_2 ($2\theta \approx 24.8^\circ$, $hkl = [111]$), LS ($2\theta \approx 27^\circ$, $hkl = [111]$) and Li_3PO_4 ($2\theta \approx 22.3^\circ$, $hkl = [110]$), it was noticed that the change of the crystalline phase formed after heat treatment steps. The calculated degree of crystallinity increased after each heat treatment step, the

crystallinity of N-0 final GC was 37%. As a result, the appearance of the materials could change significantly from the transparent glasses to translucence GCs.

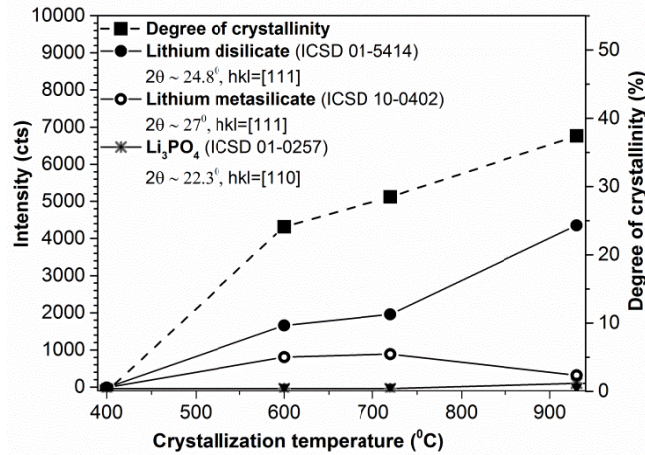


Figure 3. Illustration of the change of the crystalline phase formed after heat treatment steps.

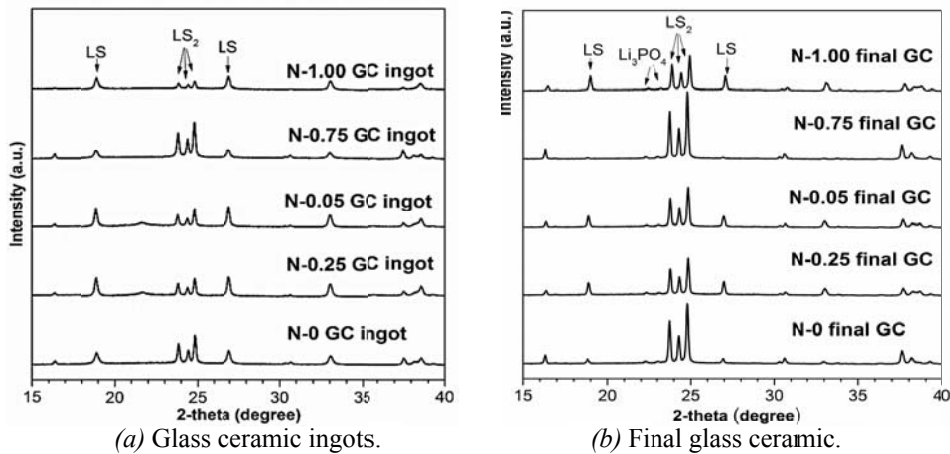


Figure 4. XRD patterns of samples with different Nd_2O_3 content.

Figure 4 is used to compare XRD patterns of GC ingots (Figure 4a) and final GCs (Figure 4b) with different Nd_2O_3 contents. Because the intensity of an X-ray diffraction pattern is directly proportional to the amount of the phase in the mixture, according to the results in Figure 4a, b, we can deduce that LS_2 in the ingot samples (after the 2-stage heat treatment at $600\text{ }^\circ\text{C}/1.5\text{ h} - 720\text{ }^\circ\text{C}/0.5\text{ h}$) was decreased when the content of Nd_2O_3 increased. Similar effect was also found in the final GCs (after being fired in hot pressing furnace at $930\text{ }^\circ\text{C}$) and LS still remained in these samples, except for the samples named N-0.75 (the intensity of main XRD peak of LS_2 in N-0.75 was higher than N-0). The semi-quantitative phase analysis of final GCs is presented in Table 3 and Figure 5. The result showed that when being heat-treated at the same conditions, the presence of Nd_2O_3 tended to reduce the crystallinity and LS_2 crystalline phase forming of final GCs, but increase the crystallite size of LS_2 from 63.6 nm to 91.8 nm (calculated for the peak at hkl [111] by equation (2)).

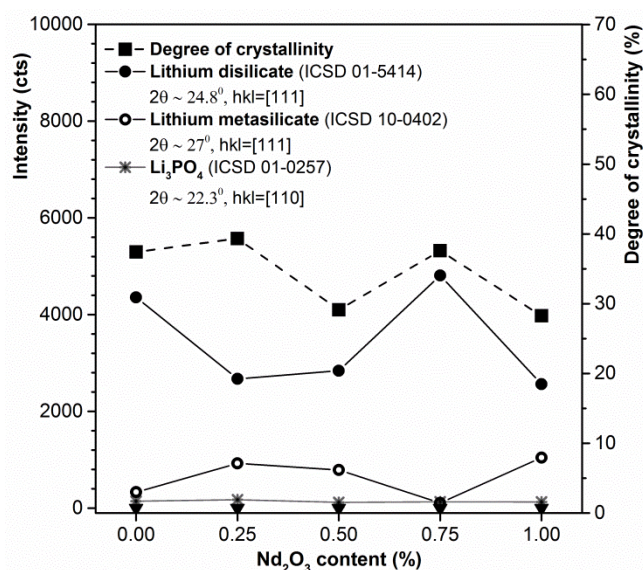


Figure 5. Dependence of crystal phases formed in final GC on Nd_2O_3 content (determined by intensities of main XRD peaks).

Table 3. Degree of crystallinity (C) and characteristic peaks of final GC containing different Nd_2O_3 content.

Sample	C (%)	Intensities of main XRD peaks (cts)			Crystallite size of LS_2 at hkl [111] (nm)
		LS_2	LS	Li_3PO_4	
N-0	37	4351	119	144	63.6
N-0.25	39	2670	57	175	56.5
N-0.50	29	2834	83	121	63.6
N-0.75	38	4802	69	131	75.2
N-1.00	28	2558	76	128	91.8

3.3. Mechanical and chemical properties

Table 4. The bending strength, Vicker hardness and chemical solubility of final GC.

Sample	3-point bending strength (MPa)	Vicker hardness (MPa)	Chemical solubility ($\mu\text{g}/\text{cm}^2$)
N-0	213±6	4738±24	27.0±0.7
N-0.25	208±4	6306±75	20.0±0.7
N-0.50	197±5	4337±20	21.7±0.4
N-0.75	293±7	5958±23	3.7±0.4
N-1.00	204±7	5349±8	20.3±0.4

The values of three-point bending strength, Vicker hardness and chemical solubility of final GCs are shown in Table 4 and Figure 6. The bending strength, the chemical solubility of the samples was decreased, the Vicker hardness was increased slightly versus the rising of the Nd_2O_3 content. Nevertheless, the N-0.75 samples were very special with the highest bending strength, the lowest chemical solubility and relative high Vicker hardness.

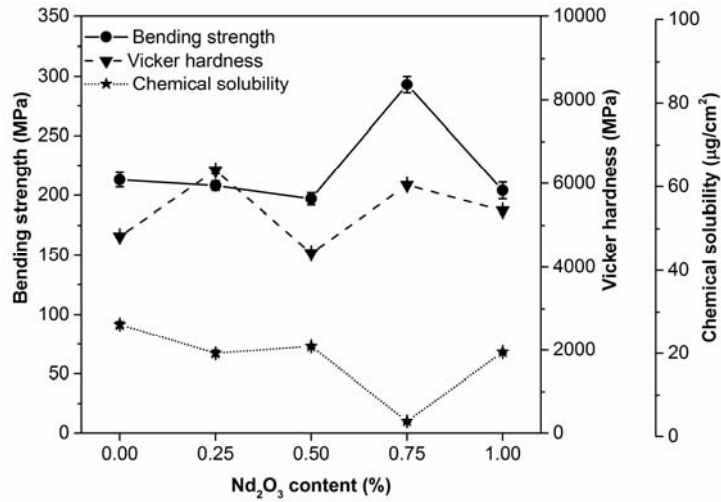


Figure 6. The properties of final GC with different Nd₂O₃ content.

3.4. Color measurements

Table 5 shows the values of CIE L*, a*, b* and the color difference, calculated by equations (3) to (6) of the final GC bars containing different Nd₂O₃-content. The color differences, ΔE*, were illustrated in Figure 7.

Table 5. The CIE L*a*b* color and the calculated color difference values of final glass ceramic bars containing different Nd₂O₃-content.

Sample	L*	a*	b*	Mean ΔL	Mean Δa	Mean Δb	Mean ΔE
N-0	88.87 ± 0.35	-7.24 ± 0.12	5.40 ± 0.01	–	–	–	–
N-0.25	85.36 ± 0.29	-6.67 ± 0.01	0.86 ± 0.06	-3.51	0.57	-4.53	5.76
N-0.50	82.36 ± 1.75	-4.77 ± 0.04	-0.70 ± 0.66	-6.51	2.47	-6.09	9.25
N-0.75	81.76 ± 2.04	-4.53 ± 0.21	-1.58 ± 0.31	-7.11	2.71	-6.98	10.32
N-1.00	79.68 ± 0.30	-4.48 ± 0.13	-2.95 ± 0.10	-9.19	2.77	-8.35	12.72

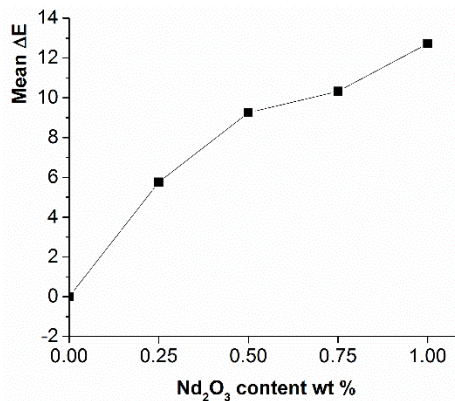


Figure 7. Effect of Nd₂O₃ additions on color difference CIE ΔE* of final GC bars which contained varying amounts of Nd₂O₃.

These results indicated that the lightness of Nd₂O₃-containing samples, L*, were significantly lower than the blank samples (N-0). The shift in reflectance in the blue range (negative b* values) and green range (negative a* values) of the spectra with different amounts of Nd₂O₃ can be observed. With increasing of the Nd₂O₃ content, the blue color increased and the green color decreased.

The color differences, ΔE^* , between the blank samples N-0 and the Nd₂O₃-containing samples, have shown that the additions of Nd₂O₃ in the range of 0 to 1.00 wt% caused the increasing of ΔE^* values from 0 to 12.72.

3.5. Microstructure

The morphology of system also was studied. Figure 8 shows the fractured surface-microstructure (non-etching, Au sputtered) of N-0 and N-0.75 final GCs. Figure 9 shows the microstructures of polished and etched surfaces of these samples.

The fractured surface-microstructure of the final GCs consisted of dispersed small plate-shaped crystals. These crystals were homogeneously dispersed in an interlocking network. They stack and overlap each other that strengthen of the GCs.

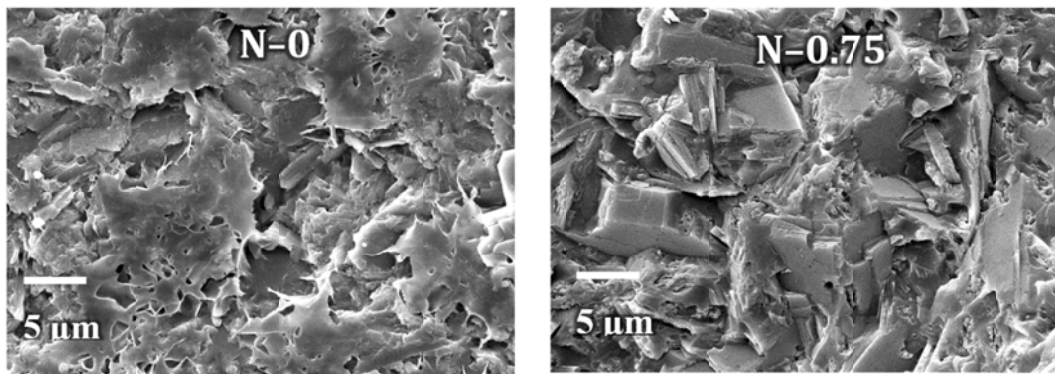


Figure 8. SEM of fractured surface of N-0 and N-0.75 final glass ceramics (non-etching, Au-sputtered).

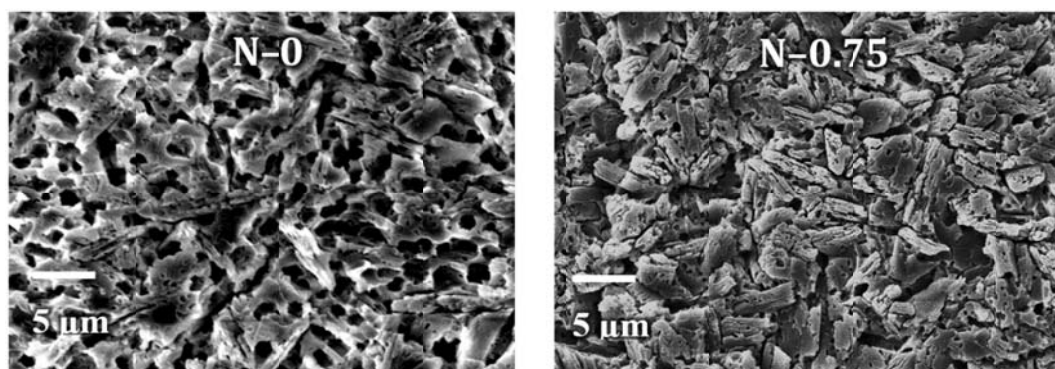


Figure 9. SEM of polished surface of N-0 and N-0.75 final glass ceramics (etched with 10%-HF for 10 s, Au-sputtered).

After etching, because the glass phase, LS crystal and Li_3PO_4 crystal were dissolved in HF solution [5], the major phase still remaining was LS_2 crystals. The LS_2 crystals with the size about of 2–5 μm can be visible. The pores as etched areas represented for LS and glass. The more closely packed and multidirectional interlocking of plate-shaped crystals in N–0.75 final GC microstructure can explain for its high bending strength, high Vicker hardness and low chemical solubility.

4. CONCLUSIONS

The effects of Nd_2O_3 content (0–1 wt%) on crystallization and the properties of GC derived from the system $\text{Li}_2\text{O}-\text{K}_2\text{O}-\text{Al}_2\text{O}_3-\text{SiO}_2-\text{P}_2\text{O}_5$ were discussed. The results showed as follows:

1. The results of DTA showed the small variation of characteristic temperatures of glass powders, especially the melting temperature T_m . It means that the GC system can be still stable under the hot–pressing process for dental restorations.
2. The main crystalline phase of final GCs was LS_2 . The chemical reaction of LS and SiO_2 had occurred to produce LS_2 . However, the degree of this reaction decreased with the rise of Nd_2O_3 content.
3. The calculated crystal sizes of LS_2 in final GCs containing Nd_2O_3 (from 63.6 nm to 91.8 nm) were larger than GC without Nd_2O_3 .
4. Nd_2O_3 made the color of final GC bars decreased green value and lightness, and increased blue value in CIEL*a*b* color space. The color differences ΔE^* increased from 0 to 12.72.
5. The samples N–0.75 had high crystallinity, the highest relative amount of LS_2 phase and the highest bending strength value.
6. Based on the study of chemical, physical, and optical properties of these GCs, we hope they can be adopted in different application such as inlays, onlays, veneers, partial or full crowns and bridges bonded to natural teeth or to implant abutments.

Acknowledgements. This research was funded by Ho Chi Minh City University of Technology, Vietnam National University – HCMC under grant number TNCS– 2015–CNVL–17. The authors also would like to thank Asst. Prof. Duangrudee Chaysuwan and her students, Dept of Materials Engineering, Faculty of Engineering Kasetsart University, Thailand.

REFERENCES

1. Holand W., Beall G. H. – Glass Ceramic Technology, John Wiley & Sons, 2012, pp. 78.
2. Tulyaganov D. U., Agathopoulos S., Kansal I., Valério P., Ribeiro M. J., Ferreira J. M. F. – Synthesis and properties of lithium disilicate glass–ceramics in the system $\text{SiO}_2-\text{Al}_2\text{O}_3-\text{K}_2\text{O}-\text{Li}_2\text{O}$, *Ceramics International* **35** (8) (2009) 3013–3019.
3. Höland W., Rheinberger V., Apel E., Van't Hoen C. – Principles and phenomena of bioengineering with glass–ceramics for dental restoration, *Journal of the European Ceramic Society* **27** (2–3) (2007) 1521–1526.
4. Goharian P., Nemati A., Shabaniyan M., Afshar A. – Properties, crystallization mechanism and microstructure of lithium disilicate glass–ceramic, *Journal of Non–Crystalline Solids* **356** (4–5) (2010) 208–214.

5. Zheng X., Wen G., Song L., Huang X. X. – Effects of P₂O₅ and heat treatment on crystallization and microstructure in lithium disilicate glass ceramics, *Acta Materialia* **56** (3) (2008) 549–558.
6. Wen G., Zheng X., Song L. – Effects of P₂O₅ and sintering temperature on microstructure and mechanical properties of lithium disilicate glass–ceramics, *Acta Materialia* **55** (10) (2007) 3583–3591.
7. Ritzberger C., Holand W., Schweiger M., Rheinberger V. – Lithium silicate glass ceramic and glass with transition metal oxide, US8759237 B2, 24–Jun–2014.
8. Rames R. H., Nestor E., Pomeroy M. J., Hampshire S. – Formation of Ln–Si–Al–O–N glasses and their properties, *Journal of the European Ceramic* **17** (15–16) (1997) 1933–1939.
9. Wang P., Yu L., Xiao H., Cheng Y., Lian S. – Influence of nucleation agents on crystallization and machinability of mica glass–ceramics, *Ceramics International* **35** (7) (2009) 2633–2638.
10. Bighetti C. M. M., Ribeiro S., S. Borges P. T., Strecker K., Machado J. P. B., Santos C. – Characterization of rare earth oxide–rich glass applied to the glass–infiltration of a ceramic system, *Ceramics International* **40** (1B) (2014) 1619–1625.
11. Wang J., Liu C., Zhang G., Xie J., Han J., Zhao X. – Crystallization properties of magnesium aluminosilicate glass–ceramics with and without rare–earth oxides, *Journal of Non–Crystalline Solids* **419** (2015) 1–5.
12. Höland W., Apel E., Van ‘t Hoen C., Rheinberger V. – Studies of crystal phase formations in high–strength lithium disilicate glass–ceramics, *Journal of Non–Crystalline Solids* **352** (38–39) (2006) 4041–4050.
13. Rukmani S. J., Brow R. K., Reis S. T., Apel E., Rheinberger V., Höland W. – Effects of V and Mn Colorants on the Crystallization Behavior and Optical Properties of Ce–Doped Li–Disilicate Glass–Ceramics, *Journal of the American Ceramic Society* **90** (3) (2007) 706–711.
14. Lindon C. J., Tranter E. G., Koppelaar W. D. – *Encyclopedia of Spectroscopy and Spectrometry*, Academic Press, 2016, pp. 728.
15. Jaffe M., Hammond W., Tolias P., Arinze T. – *Characterization of Biomaterials*, Elsevier, 2012, pp. 47.
16. Khademinia S., Alemi A., Sertkol M. – Lithium Disilicate (Li₂Si₂O₅): Mild Condition Hydrothermal Synthesis, Characterization and Optical Properties, *Journal of Nanostructures* **4** (4) (2014) 407–412.
17. International Organization for Standardization – *Dentistry: ceramic materials*, ISO 6872:2008, 2008.
18. ASTM International – *Test Method for Vickers Indentation Hardness of Advanced Ceramics*. ASTM C1327–99, 1999.
19. O’Brien J. W., Boenke M. K., Linger B. K., Groh L. C. – Cerium oxide as a silver decolorizer in dental porcelains, *Dental Materials* **14** (5) (1998) 365–369.